EurJIC
European Journal of Inorganic Chemistry

Research Article
doi.org/10.1002/ejic.202200426

Chemistry Europe
European Chemical Societies Publishing

www.eurjic.org

Comparative Analysis of a Series of pH-Responsive Sulphonated Europium Complexes for Bioassays Monitoring Acidification

Jack D. Fradgley,*[a] Matthieu Starck,[a] Laurent Lamarque,[b] and David Parker*[a]

The synthesis and photophysical evaluation of a series of hydrophilic sulphonated and pH responsive luminescent europium(III) probes are reported. The Eu emission intensities and lifetimes increase very significantly on lowering pH, leading to a 'switching on' of Eu luminescence in more acidic media. By varying the nature of the substituents at an integral aniline nitrogen atom located in the sensitising chromophore, the pK_a value of the complex can be tuned to between 4.3 and 6.3 for a set of five Eu(III) complexes. These systems are designed to allow conjugation to targeting vectors permitting, for example, the monitoring of receptor internalisation in cells. This approach can be used to tag proteins selectively and allows the monitoring of uptake into acidic organelles, enabling the creation of time-resolved internalisation assays to follow pH change in real time, both in vitro and in cellulo.

Introduction

We report the synthesis and pH dependent behaviour of a series of hydrophilic Eu(III) complexes designed for use in assays that monitor the temporal dependence of acidification.

In a eukaryotic cell, the ageing process for endosomes and phagosomes is accompanied by acidification. As endosomes mature, the pH drops from pH 6.5 to 5.5 and eventually they may evolve into lysosomes. The cytosolic pH of healthy cells is around 7.2, whilst in more mature lysosomes the pH value is around 4.5.[1] Any pH probe that it is to be used to monitor acidification needs to be designed flexibly so that the pH range from 6.5 to 4 is covered. The processes of cell surface receptor internalisation and endosomal uptake[2] are able to be monitored externally, provided that the species that is internalised (i.e. the receptor itself or its substrate) can be labelled with a non-invasive and pH sensitive dye, whose emission intensity or lifetime must vary significantly with pH over the desired range, and be amenable to accurate calibration.[3–6] Methods to study agonist induced receptor internalisation are of considerable current interest.[7,8]

We have recently created examples of europium(III) complexes that exhibit a large pH dependent change in Eu emission lifetime. The emission intensity increases by around two orders of magnitude on acidification, and has been examined using a variety of time-gated acquisition methods.[9,10] Each of these Eu(III) complexes, e.g. [**Eu.*L*^{1}**] and [**Eu.*L*^{2}**] (Figure 1), contains a strongly absorbing alkynyl-aryl chromophore, with the latter example having a brightness of 10,200 M^{-1} cm^{-1} (332 nm) at pH 4, and a Eu emission lifetime of 0.84 ms. With a conjugated diethylamino group the pK_a value is 6.2 (295 K) and falls by about one unit when a methyl group replaces one of the ethyl substituents.[9,10] The absorption spectrum changes with pH because acidification perturbs the energy of the ligand centred and internal charge transfer transitions that exist in these EuroTracker™ dyes and several structurally related series of complexes.[11–18]

In order to avoid such complexes binding non-specifically to proteins or other macromolecules, we have introduced water solubilising sulphonate groups on the ligand periphery, e.g. [**Eu.*L*^{3a,b}**]. These two examples were functionalised via the phenolic oxygen atom.[10] In this work, the scope and utility of the range of Eu(III) complexes is expanded to cover the full range of pH. We report the synthesis and compare the pH dependent luminescence behaviour of structurally related complexes, [**Eu.*L*^{4a,4b}**] and [**Eu.*L*^{5}**], where the site of sulphonation is introduced by functionalising the aniline nitrogen atom. In each case, in the synthetic approach we have taken advantage of a 2,2,2-trifluoroethyl protecting group for the sulphonate moiety, unmasking the anion under strongly basic aqueous conditions in the final step of the ligand synthesis.[19]

Results and Discussion

Ligand and complex synthesis

Mono-alkylation of 3-amino-4-methoxy-iodobenzene with the 3-bromopropyl- sulphonate ester, **1**, proceeded in 63% yield to

[a] Dr. J. D. Fradgley, Dr. M. Starck, Prof. D. Parker
Department of Chemistry, Durham University,
South Road, Durham DH1 3LE, UK
E-mail: j.d
E-mail: fradgley@dur.ac.uk
david.parker@dur.ac.uk
[b] Dr. L. Lamarque
Perkin Elmer Bioassays,
BP 84175, 30200 Codolet, France

Supporting information for this article is available on the WWW under https://doi.org/10.1002/ejic.202200426

Research Article
doi.org/10.1002/ejic.202200426

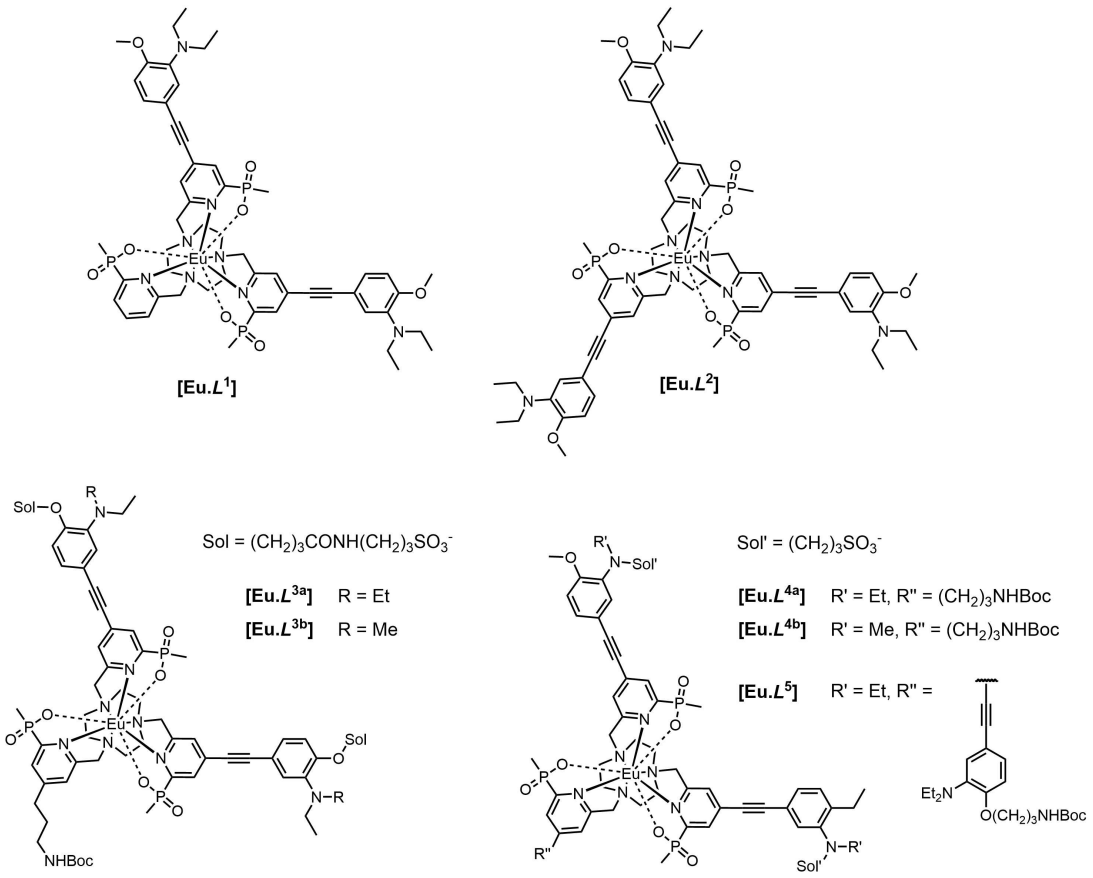

Figure 1. Structures of Eu(III) complexes exhibiting pH dependent emission.

give the secondary amine **2**, (Scheme 1). A stepwise reductive amination reaction, using either acetaldehyde or paraformaldehyde, allowed the isolation of their N-ethyl and N-methyl derivatives, **3a** and **3b**, in 75 and 90% isolated yields, respectively. Palladium catalysed coupling with trimethylsilylacetylene afforded the alkynes **4a** and **4b**, whose silyl group was removed by fluoride before a second Pd-catalysed coupling of **5a** or **5b** with the 4-bromopyridine derivative, **6**, in

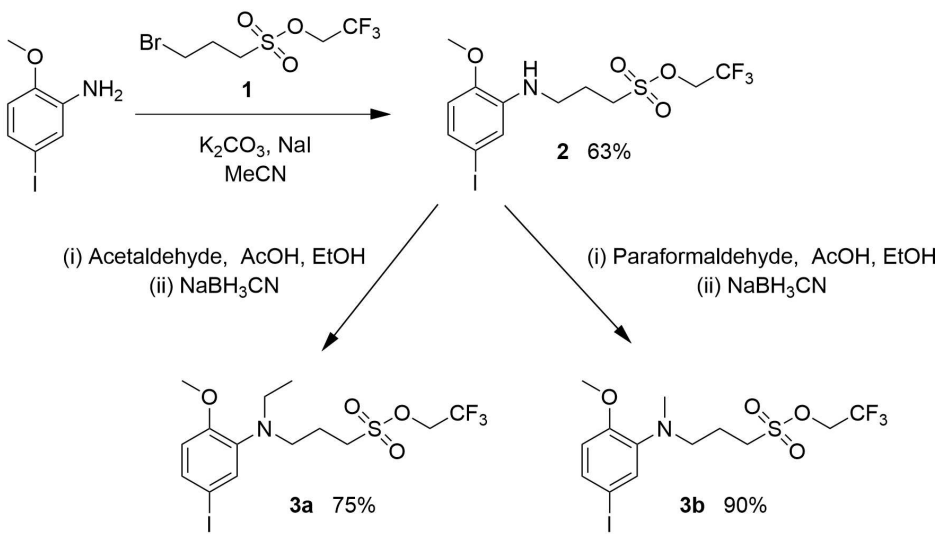

Scheme 1. Synthesis of the trifluoroethyl sulphonate esters, **3a** and **3b**

Research Article
doi.org/10.1002/ejic.202200426

MeCN (Scheme 2) allowed the isolation of the alcohols, **7a** and **7b**, from which the mesylate esters, **8a** and **8b** were derived.

The final steps of the synthesis of ***L*[5]** and ***L*[4a/4b]** were undertaken in a similar manner from mono-Boc-1,4,7-triazacyclononane (SI) involving some common or previously reported intermediates, e.g. **6**, **11** and **12** (Figure 2).[9,10,17]

Each synthetic sequence comprised a stepwise series of ring *N*-alkylation and de-protection reactions. The Boc removal step involved strongly acidic conditions, but protonation of the aryl dialkylamino group electrostatically inhibited the unwanted, competitive acid catalysed alkyne hydration. Following hydrolysis of the ester and sulphonate groups in aqueous methanolic solution, the corresponding Eu(III) complexes were prepared after adjusting the pH to 6. Each complex was purified by reverse phase HPLC. A representative example of the approach is given here (Scheme 3) for ***L*[4a/4b]**; further details can be found in the SI.

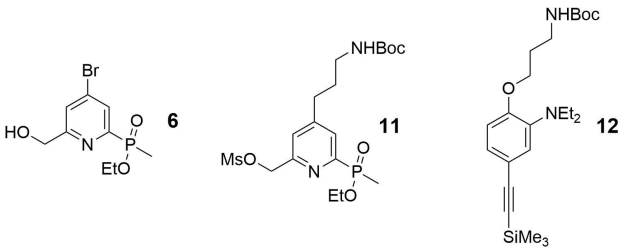

Figure 2. Previously reported synthetic intermediates used within this work.

Absorption spectral variation with pH

Lowering the pH of an aqueous solution of each Eu complex gave rise to a hypsochromic shift of the main UV-visible spectral absorbance band, accompanied by a slight increase in absorbance, (Figure 3). The overall changes in the absorption spectrum with pH observed for the complexes [**Eu.*L*[4a,4b]**] were very similar to those found for the dichromophore series of complexes [**Eu.*L*[2,3a,3b]**]. The variations in absorbance with pH were characterised by the occurrence of isosbestic points at 332 nm for [**Eu.*L*[4a]**], and at 280 and 336 nm for [**Eu.*L*[4b]**], respectively. The N-ethyl functionalised examples, in each set of complexes, differed from the N-methyl analogues in displaying only a single isosbestic point.

Interestingly, examination of the absorption *vs.* pH behaviour for the trichromophore complex [**Eu.*L*[5]**] revealed two isosbestic points at 280 and 332 nm (Figure 3), in contrast to the behaviour of the parent trichromophore complex [**Eu.*L*[2]**] for which no well-defined isosbestic point had been observed. Whilst the absorbance-pH profile (hypsochromic shift, intensity increase) was mirrored by [**Eu.*L*[5]**], the relative increase in absorbance on acidification was lower, compared to the series of dichromophore complexes.

pH Variation of Eu emission and excitation spectra

Following excitation at the isosbestic wavelength, the spectral form of Eu luminescence observed for [**Eu.*L*[4a,4b,5]**] was identical to that found with [**Eu.*L*[3a,3b]**]. This lack of change is predictable, given that the structural changes in the ligand occur away from the immediate coordination environment of the europium(III)

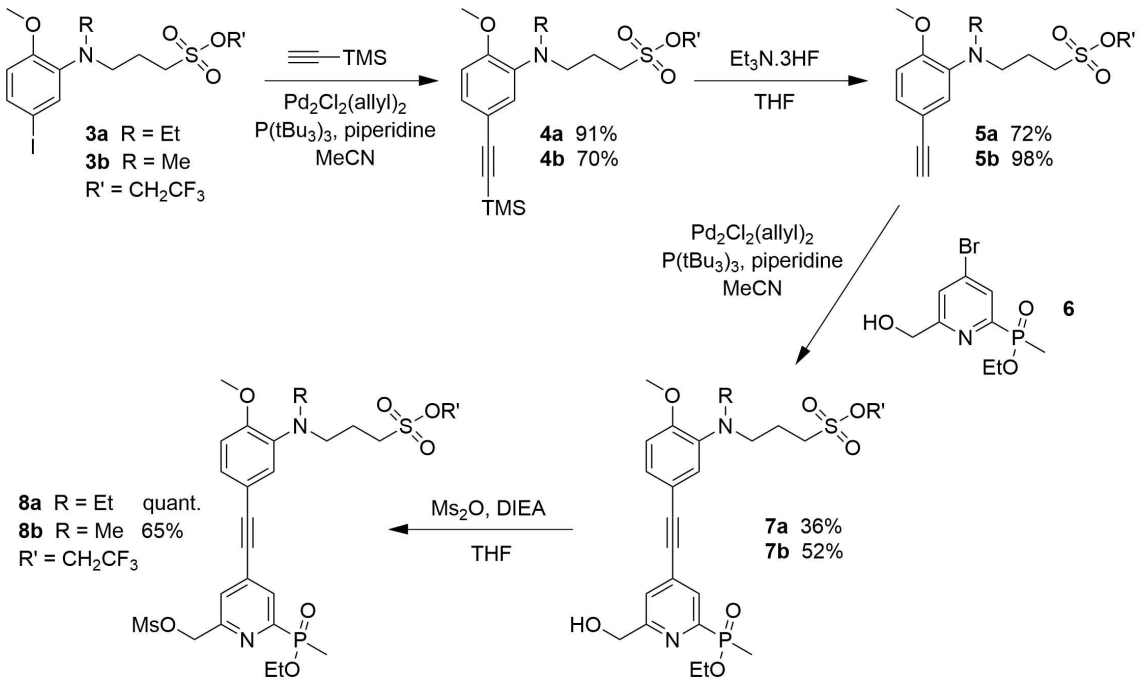

Scheme 2. Synthesis of the mesylates, **8a** and **8b**.

Research Article
doi.org/10.1002/ejic.202200426

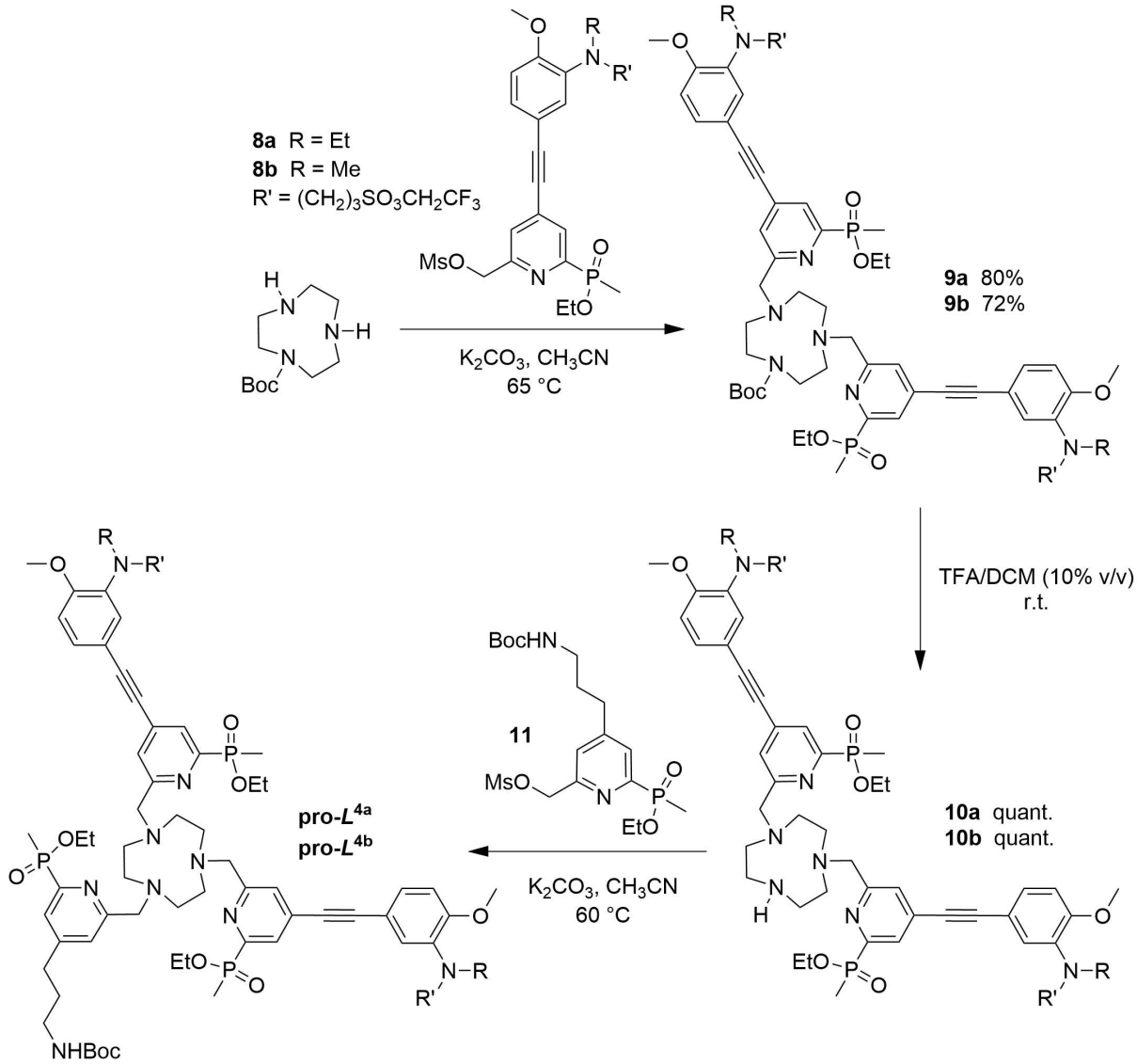

Scheme 3. Synthesis of the pro-ligands L^{4a} and L^{4b}.

ion. A large increase in europium emission intensity on acidification was observed in every case, with 'switch-on' ratios of 925, 1040 and 1360 for [**Eu.*L*^{4a,4b,5}**], respectively. It is noted that this ratio for the methyl analogue, [**Eu.*L*^{4b}**], was calculated between pH 7 and 3, owing to its lower inherent pK_a, whereas values for [**Eu.*L*^{4a,5}**] were calculated between pH 8 and 4.

As the pH was lowered, each complex displayed an excitation spectrum that increased in intensity, without variation of spectral form. Thus, it is the emissive protonated complex that is being observed across the pH range. Some variation in excitation spectral form *between* different complexes was evident, however. In the case of [**Eu.*L*^{4b}**] for example, a very broad profile was obtained with no distinctive features. In contrast, the overall broad profile displayed by the ethyl analogue, [**Eu.*L*^{4a}**] featured two clearly overlapping bands centred at 286 and 331 nm. These bands become more evident under more acidic conditions, notwithstanding the breadth of the profile. Finally, the tri-chromophore complex [**Eu.*L*^{5}**] displayed a similar excitation profile to that of [**Eu.*L*^{4a}**], with two distinct bands at 281 and 338 nm, in which the band at longer wavelength was the more well-defined, (Figure 4).

pH Dependence of Eu emission lifetime

The variation of the europium emission lifetime with pH in 0.1 M NaCl was probed for the complexes [**Eu.*L*^{4a,4b,5}**], allowing a comparison with behaviour reported for the structurally related Eu complexes of $L^{3a,3b}$. The resulting sigmoidal curves were fitted by iterative non-linear least-squares methods of analysis to allow an estimate of the pK_a values, (Figure 5). Inspection of the curves clearly demonstrates the impact of substituting an ethyl for a methyl group, and the pK_a value decreased by approximately 0.9 units, from 5.21 to 4.32. The upper and lower

Research Article
doi.org/10.1002/ejic.202200426

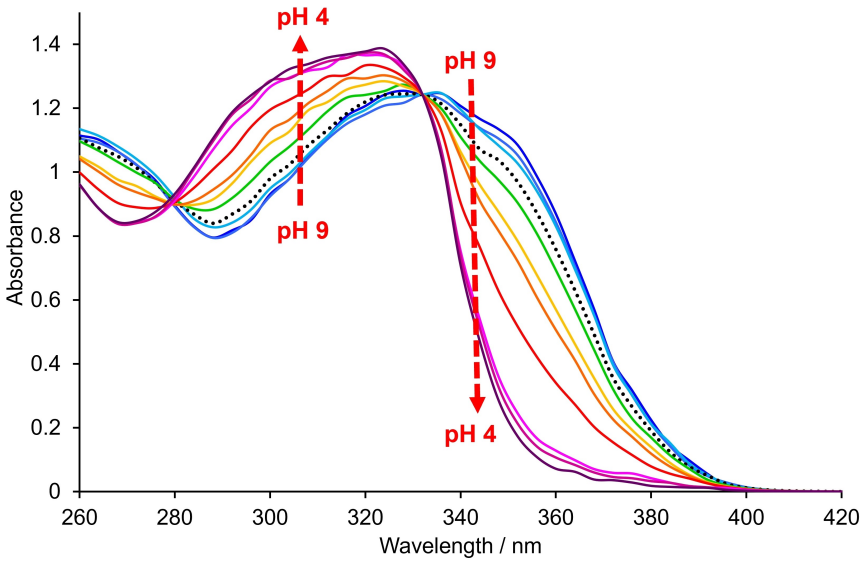

Figure 3. Variation of the absorption spectrum of [**Eu.*L*^{5}**] with pH, revealing isosbestic points at 280 and 332 nm (295 K, 0.1 M NaCl). The absorbance profile at pH 7 is indicated with black dots.

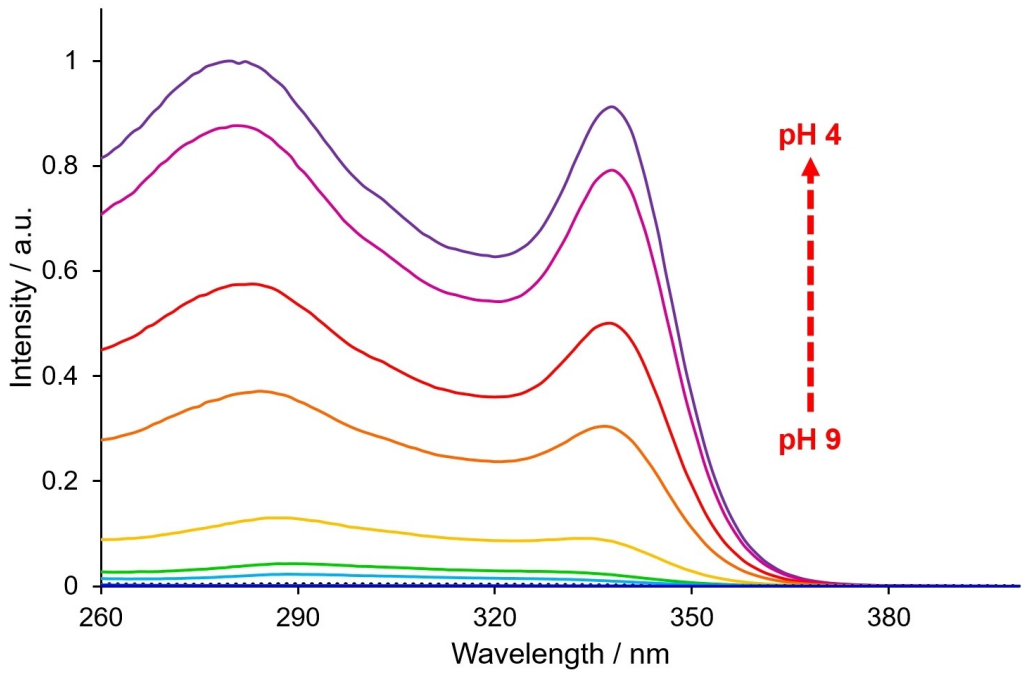

Figure 4. pH Variation of the excitation spectrum of [**Eu.*L*^{5}**] (λ_{em} 613 nm, 295 K, $c_{complex}$ = 15 μM, 0.1 M NaCl). The excitation spectrum at pH 7 is shown with black dots (near baseline).

limiting lifetime values did not vary significantly. On acidification, the observed europium emission lifetime was enhanced by 248, 226 and 390% for [**Eu.*L*$^{4a-b,5}$**], respectively. For each europium(III) complex, the measured lifetime was independent of complex concentration from 2 to 50 μM, and did not vary on degassing the solution, in both acidic and basic media.

The rate of proton transfer to and from N in water (typically 10^{10} s^{-1}) occurs faster than both the rate of decay of the excited europium ion (ca. 10^3 s^{-1}) and the rate of decay of intermediate ligand ICT or triplet excited states. Now, the rate of electron transfer from the nitrogen lone pair orbital to an excited Eu ion is also normally faster than the rate of energy transfer that leads to population of the Eu* $^5D_0$ state, and is also much faster than the radiative rate of decay of the Eu excited state.[20,21] Therefore,

Research Article
doi.org/10.1002/ejic.202200426

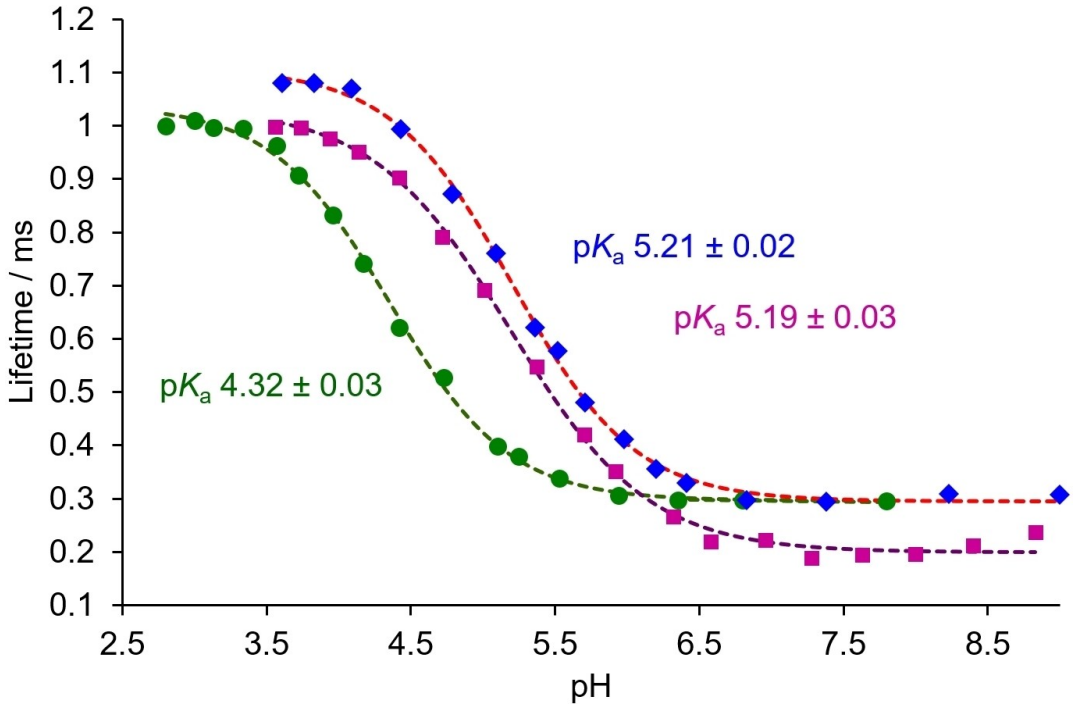

Figure 5. Variation of the europium emission lifetime with pH for [**Eu.*L*^{4a,4b,5}**] (blue diamonds, green circles, and purple squares, respectively, λ_{em} 613 nm, 295 K, $c_{complex}$ = 15 μM, 0.1 M NaCl). The experimental data was fitted using non-linear, least squares methods of regression analysis (dashed lines).

during the millisecond lifetime of the Eu* $^5D_0$ excited state, over the pH range 4 to 8, deprotonation of the amine group occurs millions of times, so that fast electron transfer can occur from the unprotonated chromophore moiety to the Eu ion, quenching the Eu excited state and thereby shortening the observed 'time-averaged' emission lifetime. Consistent with this hypothesis, the same pH dependence of the Eu emission lifetime was observed for each complex following *direct* excitation of the Eu ion at 397 nm, indicating that it is the Eu $^5D_0$ excited state that is quenched by charge transfer and not any intermediate, shorter-lived ligand excited state.

Summary and Conclusions

The photophysical properties of five hydrophilic sulphonated europium(III) complexes can be compared to those reported for the more lipophilic analogues, [**Eu.*L*^{1}**] and [**Eu.*L*^{2}**], (Table 1).

Values are given for the molar extinction coefficients, ***ε***, and the overall emission quantum yields, φ. Each complex was excited at the isosbestic point where that was present. For each of the di-chromophore series of complexes, ***ε*** values were estimated assuming the Beer-Lambert Law and were found to be consistent for structural analogues, *e.g.* [**Eu.*L*^{3a,3b}**], with values in the range 35,000–39,000 M^{-1} cm^{-1}. On examining the

Table 1. Salient photophysical properties of europium(III) complexes (295 K, 0.1 M NaCl).

Complex	λ_{exc} [nm]	ε[a] [$M^{-1}cm^{-1}$]	τ [ms]	Φ[a] [%]	q	B[a] [$M^{-1}cm^{-1}$]
[**Eu.*L*^{1}**]	328	35,000	0.34[b] 1.00[c]	0.2[b] 17.6[c]	0	70[b] 6,160[c]
[**Eu.*L*^{3a}**]	332	39,000	0.26[b] 1.02[c]	0.3[b] 16.0[c]	0	117[b] 6,240[c]
[**Eu.*L*^{3b}**]	332	39,000	0.28[b] 1.04[c]	0.01[b] 15.0[c]	0	4[b] 5,850[c]
[**Eu.*L*^{4a}**]	332	35,000	0.31[b] 1.08[c]	0.06[b] 13.4[c]	0	21[b] 4,690[c]
[**Eu.*L*^{4b}**]	336	35,000	0.31[d] 1.01[e]	0.06[d] 13.0[e]	0	21[d] 4,550[e]
[**Eu.*L*^{2}**]	331	46,000 60,000	0.25[b] 0.84[c]	0.1[b] 17.0[c]	0	46[b] 10,200[c]
[**Eu.*L*^{5}**]	332	75,000	0.20[b] 0.98[c]	0.01[b] 15.9[c]	0	8[b] 11,925[c]

[a] Parameter calculated at the stated excitation wavelength, which is an isosbestic point where appropriate. [b] Values at pH 8. [c] Values at pH 4. [d] Values at pH 7. [e] Values at pH 3. Experimental errors of emission lifetime and overall quantum yield are ±5 and 15%, respectively.

Research Article
doi.org/10.1002/ejic.202200426

complex [**Eu.*L*^{5}**], a higher ε value of 75,000 $M^{-1}cm^{-1}$ was estimated, greater than that found for the related complex [**Eu.*L*^{2}**]. For each complex, the Φ values tended to zero at the high pH limit, increasing to 13–16% at the low pH limit. These values are similar to those determined for the di- and tri-chromophore parent complexes [**Eu.*L*^{1,2}**], respectively.

With these two parameters determined, an estimation of complex brightness, *B*, can be made. Whilst the first set of complexes, [**Eu.*L*^{3a,3b}**], display comparable brightness values to the parent [**Eu.*L*^{1}**], a reduction in brightness of 20% was observed for [**Eu.*L*^{4a,4b}**], relative to the other di-chromophore complexes. In contrast, an increased brightness value was estimated for [**Eu.*L*^{5}**], relative to [**Eu.*L*^{2}**].

Thus, by varying the nature of the nitrogen substituents, the pK_a value can be varied significantly compared to those found for [**Eu.*L*^{1,2}**], with values ranging from 4.32(03)–6.18(05) in 0.1 M NaCl, (Table 2). The pK_a values found for this set of five complexes cover just over two pH units, and hence are tuned to the range found both in early and mature endosomes and in more acidic lysosomes.

Substitution of one ethyl group at nitrogen by a methyl reduced the pK_a value by approximately 0.8–0.9 (*c.f.* [**Eu.*L*^{3a,3b}**]), in accord with the more favourable solvation of the protonated form and the stronger NCH:::O hydrogen bonding interactions for the less sterically bulky N–Me complex. Additionally, by replacing one of the N-ethyl groups with an N-substituted propylsulfonate moiety, the pK_a value also reduced by approximately one unit. Such a decrease occurred for both the N-ethyl and the N-methyl complex pairs.

The protonation behaviour of the N-substituted sulphonated complexes may be rationalised by considering three contributing factors. First, it is reasonable to assume that following protonation of the amino nitrogen, the presence of the anionic charge in close proximity to the positive charge will stabilise the protonated form through a favourable field effect. Here, the protonated species is a zwitterion. The electrostatic stabilisation of the protonated form, *i.e.* the conjugate acid, leads to an increase in the pK_a value accordingly. Furthermore, a weak σ-polarisation effect created by the electron-withdrawing alkylsulphonate moiety tends to reduce electron density at the N atom in the conjugate base. The degree of σ-bond polarisation is distance-dependent and the length of the propyl chain needs to be taken into consideration when considering the significance of this effect. Overall, it is reasonable to hypothesise that the reduced basicity of the free base and the increase in the stability of the protonated form both contribute to the observed pK_a decrease.

A third factor to consider is the nature and extent of solvation of the N-protonated form of the conjugate acid, and the perturbation of the local hydration sphere created by the presence of the proximate charged sulphonate group. In the absence of this anion, solvation of the protonated complex is expected to stabilise the conjugate acid, for example by directed H-bonding involving an NH donor and a solvent water oxygen acceptor. The localisation of negative charge on each oxygen atom of the sulphonate group gives rise to a relatively ordered local solvation structure. Indeed, sulphonate anions are often described as kosmotropes.[22–28] Given the significantly greater hydration free energies of anions compared to relatively lipophilic (chaotropic) ammonium cations, it is plausible that the relative free energy of solvation of the N-protonated species compared to the unprotonated form is less favourable in the presence of the neighbouring sulphonate group. Such a differential solvation effect could be significant and is likely to be associated with part of the overall increase in the acidity of the sulphonated complex species.

In conclusion, the relationship between probe structure and the pH dependent behaviour of a series of five hydrophilic Eu(III) complexes has been investigated in detail. With pK_a values that vary between 6.3 and 4.3, the key pH range found in acidification processes in cells and in vitro is covered, so that a particular Eu complex can be selected from this family, according to its projected use in assays that require the monitoring of the temporal dependence of acidification.

Table 2. Summary of pK_a values determined in the stated media; the top 5 entries refer to systems with two chromophores; the last two entries possess three.

Complex	Conditions	pK_a[a]
[**Eu.*L*^{1}**]	0.1 M NaCl	6.30 (05)
	NIH-3T3 cell lysate	6.25 (05)
[**Eu.*L*^{3a}**]	0.1 M NaCl	6.18 (03)
	NIH-3T3 cell lysate	6.00 (04)
[**Eu.*L*^{3b}**]	0.1 M NaCl	5.34 (03)
[**Eu.*L*^{4a}**]	0.1 M NaCl	5.21 (02)
[**Eu.*L*^{4b}**]	0.1 M NaCl	4.32 (03)
[**Eu.*L*^{2}**]	0.1 M NaCl	6.21 (05)
	NIH-3T3 cell lysate	5.92 (05)
[**Eu.*L*^{5}**]	0.1 M NaCl	5.19 (03)

[a] pK_a values (295 K) are the mean of three replicates, with experimental errors in parenthesis.

Experimental Information

General Procedures. Commercially available reagents were used as received. Solvents were laboratory grade and were dried over appropriate drying agents when required. Where appropriate, solvents were degassed using freeze-pump-thaw cycles. Thin layer chromatography (TLC) was carried out on aluminium-backed silica gel plates with 0.2 mm thick silica gel 60 F254 (Merck), and visualised by UV irradiation at 254 nm or 366 nm. Preparative flash column chromatography was performed using flash silica gel 60 (230–400 mesh) from Merck or Fluorochem. ^{1}H, ^{13}C, ^{19}F, ^{29}Si, and ^{31}P NMR spectra were recorded in commercially available deuterated solvents on a Bruker Avance-400 (^{1}H at 400.06 MHz, ^{13}C at 100.61 MHz, ^{19}F at 376.50 MHz, ^{29}Si at 79.49 MHz, and ^{31}P at 161.95 MHz), a Mercury 400 (^{1}H at 399.95 MHz), a Varian V NMRS-600 (^{1}H at 599.67 MHz, ^{13}C at 150.79 MHz, and ^{31}P at 242.75 MHz), or a Varian V NMRS-700 (^{1}H at 699.73 MHz, ^{13}C at 175.95 MHz, and ^{31}P at 283.26 MHz). All chemical shifts are in ppm and coupling constants are in Hz. Electrospray mass spectra were obtained on a TQD mass spectrometer equipped with an Acquity UPLC system, an electrospray ion source, and an Acquity photodiode array detector (Waters Ltd., UK). Accurate masses were recorded on an LCT Premier XE mass spectrometer or a QToF Premier Mass spectrometer, both equipped with an Acquity UPLC, a lock-mass electrospray ion source, and an Acquity photodiode array detector (Waters Ltd., UK). Methanol or acetonitrile were used as the carrier solvents.

HPLC Analysis. Reverse phase HPLC (RP-HPLC) was carried out at 295 K using a Shimadzu system consisting of a Degassing Unit (DGU-20A5R), a Prominence Preparative Liquid Chromatography pump (LC-20AP), a Prominence UV-Vis Detector (SPD-20A) and a Communications Bus Module (CBM-20A). For the preparative HPLC, an XBridge C_{18} OBD column was used (19×100 mm, 5 μm) with a flow rate of 17 mL min^{-1}. For analytical HPLC, a Shimadzu Shim-Pack VP-ODS column (4.6×150 mm, 5 μm) was used with a flow rate of 2.0 mL min^{-1}. The solvent system and gradient used to achieve purification is specified within the SI.

Optical Measurements. All solution state optical analyses were carried out in quartz cuvettes with a path length of 1 cm. UV-Vis absorbance spectra were measured on an ATI Unicam UV-Vis spectrometer (Model UV2) using Vision software (version 3.33). Emission spectra were recorded using either an ISA Jobin-Yvon Spex Fluorolog-3 luminescence spectrometer using DataMax software (version 2.2.10) or a HORIBA Jobin-Yvon Fluorolog-3 luminescence spectrometer equipped with an iHR320 module, which selects either a HORIBA FL-1073 (Hamamatsu R928P) photomultiplier tube or a HORIBA Synapse BIDD CCD for detection of emitted light, using FluorEssence software (based on Origin® software). Quantum yields were recorded against the reference standard $[Ru(bipy)_3]Cl_2$. Molar extinction coefficients were determined at the stated wavelength utilising absorbance measurements at varying complex concentrations (Beer-Lambert law). Brightness values were estimated as the product of the experimentally determined quantum yields and molar extinction coefficients ($B = \Phi \times \varepsilon$). Lifetime measurements were made using a Perkin Elmer LS55 spectrometer using FL Winlab software.

Acknowledgements

We thank EPSRC (EP/L01212X/1) for grant and partial studentship support (JDF.

Conflict of Interest

The authors declare no conflict of interest.

Data Availability Statement

The data that support the findings of this study are available in the supplementary material of this article.

Keywords: Europium · Luminescence · pH-responsive complexes · Photophysics · Sensors

[1] J. R. Casey, S. Grinstein, J. Orlowski, *Nat. Rev. Mol. Cell Biol.* **2010**, *11*, 50–61.
[2] M. Kaksonen, A. Roux, *Nat. Rev. Mol. Cell Biol.* **2018**, *19*, 313–326.
[3] Y. Urano, D. Asanuma, Y. Hama, Y. Koyama, T. Barrett, M. Kamiya, T. Nagano, T. Watanabe, A. Hasegawa, P. L. Choyke, H. Kobayashi, *Nat. Med.* **2009**, *15*, 104–109.
[4] D. Asanuma, Y. Takaoka, S. Namiki, K. Takikawa, M. Kamiya, T. Nagano, Y. Urano, K. Hirose, *Angew. Chem. Int. Ed.* **2014**, *53*, 6085–6089; *Angew. Chem.* **2014**, *126*, 6199–6203.
[5] A. Grover, B. F. Schmidt, R. D. Salter, S. C. Watkins, A. S. Waggoner, M. P. Bruchez, *Angew. Chem. Int. Ed.* **2012**, *51*, 4838–4842; *Angew. Chem.* **2012**, *124*, 4922–4926.
[6] M. Isa, D. Asanuma, S. Namiki, K. Kumagai, H. Kojima, T. Okabe, T. Nagano, K. Hirose, *ACS Chem. Biol.* **2014**, *9*, 2237–2241.
[7] a) D. Donnelly, *Br. J. Pharmacol.* **2012**, *166*, 27–41; b) S. N. Roed, P. Wismann, C. R. Underwood, N. Kulahin, H. Iversenn, K. A. Cappelen, L. Schäffer, J. Lehtonen, J. Hecksher-Soerensen, A. Secher, J. M. Mathiesen, H. Bräuner-Osborne, J. L. Whistler, S. M. Knudsen, M. Waldhoer, *Mol. Cell. Endocrinol.* **2014**, *382*, 938–949.
[8] W. J. C. van der Velden, F. X. Smit, C. B. Christiansen, T. C. Møller, G. M. Hjortø, O. Larsen, S. P. Schiellerup, H. Bräuner-Osborne, J. J. Holst, B. Hartmann, T. M. Frimurer, M. M. Rosenkilde, *ACS Pharmacol. Transl. Sci.* **2021**, *4*, 296–313, https://www.ncbi.nlm.nih.gov/pmc/articles/PMC7887852/.
[9] M. Starck, J. D. Fradgley, R. Pal, J. M. Zwier, L. Lamarque, D. Parker, *Chem. Eur. J.* **2021**, *27*, 766–777.
[10] J. D. Fradgley, M. Starck, M. Laget, E. Bourrier, E. Dupuis, L. Lamarque, E. Trinquet, J. M. Zwier, D. Parker, *Chem. Commun.* **2021**, *57*, 5814–5817.
[11] M. Soulié, F. Latzko, E. Bourrier, V. Placide, S. J. Butler, R. Pal, J. W. Walton, P. L. Baldeck, B. Le Guennic, C. Andraud, J. M. Zwier, L. Lamarque, D. Parker, O. Maury, *Chem. Eur. J.* **2014**, *20*, 8636–8646.
[12] S. J. Butler, M. Delbianco, L. Lamarque, B. K. McMahon, E. R. Neil, R. Pal, D. Parker, J. W. Walton, J. M. Zwier, *Dalton Trans.* **2015**, *44*, 4791–4803.
[13] M. Starck, R. Pal, D. Parker, *Chem. Eur. J.* **2016**, *22*, 570–580.
[14] S. J. Butler, L. Lamarque, R. Pal, D. Parker, *Chem. Sci.* **2014**, *5*, 1750–1756.
[15] S. Shuvaev, M. Starck, D. Parker, *Chem. Eur. J.* **2017**, *23*, 9974–9989.
[16] M. Delbianco, V. Sadovnikova, E. Bourrier, G. Mathis, L. Lamarque, J. M. Zwier, D. Parker, *Angew. Chem. Int. Ed.* **2014**, *53*, 10718–10722; *Angew. Chem.* **2014**, *126*, 10894–10898.
[17] J. W. Walton, R. Carr, N. H. Evans, A. M. Funk, A. M. Kenwright, D. Parker, D. S. Yufit, M. Botta, S. De Pinto, K.-L. Wong, *Inorg. Chem.* **2012**, *51*, 8042–8056.
[18] M. Starck, J. D. Fradgley, S. Di Vita, J. A. Mosely, R. Pal, D. Parker, *Bioconjugate Chem.* **2020**, *31*, 229–240.
[19] M. Delbianco, L. Lamarque, D. Parker, *Org. Biomol. Chem.* **2014**, *12*, 8061–8071.
[20] D. Parker, J. D. Fradgley, K.-L. Wong, *Chem. Soc. Rev.* **2021**, *50*, 8193–8213.
[21] M. W. Mara, D. S. Tatum, A.-M. March, G. Doumy, E. G. Moore, K. N. Raymond, *J. Am. Chem. Soc.* **2019**, *141*, 11071–11081.
[22] K. D. Collins, *Biophys. J.* **1997**, *72*, 65–76.
[23] B. Hribar, N. T. Southall, V. Vlachy, K. R. Dill, *J. Am. Chem. Soc.* **2002**, *124*, 12302–12311.
[24] R. M. Lynden-Bell, P. G. Debenedetti, *J. Phys. Chem. B* **2005**, *109*, 6527–6534.
[25] R. M. Lynden-Bell, J. C. Rasaiah, *J. Chem. Phys.* **1997**, *107*, 1981–1991.
[26] S. Kaneshan, S. H. Lee, R. M. Lynden-Bell, J. C. Rasaiah, *J. Phys. Chem. B* **1998**, *102*, 4193–4204.
[27] A. L. Thompson, D. Parker, D. A. Fulton, J. A. K. Howard, S. U. Pandya, H. Puschmann, K. Senanayake, P. A. Stenson, A. Badari, M. Botta, S. Avedano, S. Aime, *Dalton Trans.* **2006**, 5605–5616.
[28] E. A. Krestov, Thermodynamics of Solvation: Solution and Dissolution, Ions and Solvents, Structure and Energetics, Horwood, New York, **1991**.

Manuscript received: July 4, 2022
Revised manuscript received: July 21, 2022